

Mutations of *VMD2* Splicing Regulators Cause Nanophthalmos and Autosomal Dominant Vitreoretinopathopathy (ADVIRC)

Jill Yardley,^{1,2} Bart P. Leroy,^{2,3,4} Niki Hart-Holden,^{1,2} Bart A. Lafaut,⁵ Bart Loeys,⁴ Ludwine M. Messiaen,⁴ Rabat Perveen,¹ M. Ashwin Reddy,⁶ Shomi S. Bhattacharya,⁶ Elias Traboulsi,⁷ Diana Baralle,⁸ Jean-Jacques De Laey,³ Bernard Puech,⁹ Philippe Kestelyn,³ Anthony T. Moore,⁶ Forbes D. C. Manson,^{1,10,11} and Graeme C. M. Black^{1,2,10,11}

PURPOSE. To investigate the genetic basis of autosomal dominant vitreoretinopathopathy (ADVIRC), a rare, inherited retinal dystrophy that may be associated with defects of ocular development, including nanophthalmos.

METHODS. A combination of linkage analysis and DNA sequencing in five families was used to identify disease-causing mutations in *VMD2*. The effect of these mutations on splicing was assessed using a minigene system.

RESULTS. Three pathogenic sequence alterations in *VMD2* were identified in five families with nanophthalmos associated with ADVIRC. All sequences showed simultaneous missense substitutions and exon skipping.

CONCLUSIONS. *VMD2* encodes bestrophin, a transmembrane protein located at the basolateral membrane of the RPE, that is also mutated in Best macular dystrophy. We support that each heterozygous affected individual produces three bestrophin isoforms consisting of the wild type and two abnormal forms: one containing a missense substitution and the other an in-frame deletion. The data showed that *VMD2* mutations caused

defects of ocular patterning, supporting the hypothesized role for the RPE, and specifically *VMD2*, in the normal growth and development of the eye. (*Invest Ophthalmol Vis Sci.* 2004;45:3683-3689) DOI:10.1167/iov.04-0550

The retinal pigment epithelium (RPE) is a cellular monolayer interlinked with photoreceptor outer segments that is critical for mammalian retinal development and maintenance. Early ablation of the RPE leads to the arrest of eye growth and subsequent resorption of all ocular structures.¹ In addition, developmental disorders including microphthalmia can result from mutations in RPE-specific genes such as the murine microphthalmia-associated transcription factor *Mitf*.² The RPE is also important for normal photoreceptor function in postnatal life. It performs an essential role in regulating the transport of nutrients and waste products to and from the retina, is involved in the phagocytosis of shed outer segments, and is important in maintaining homeostasis of the outer retina.³

A number of inherited retinal disorders are caused by mutations in genes expressed in the RPE. One example, Best disease or vitelliform macular dystrophy (*VMD2*, MIM 153700), is an autosomal dominant disorder associated with macular visual loss in late adolescence or adulthood caused by mutations in the *VMD2* gene.⁴ The gene product, bestrophin, is a 585 amino acid transmembrane protein located at the basolateral membrane of the RPE that acts as an oligomeric chloride channel.⁵ Bestrophin mutations alter chloride ion-related conductance across the RPE cell membrane,^{5,6} and abnormal channel function may explain the abnormal electro-oculogram (EOG) seen in patients with Best disease. Almost all *VMD2* sequence alterations in patients with classical Best disease are missense mutations (www.uni-wuerzburg.de/humangenetics/vmd2.html and Ref. 7).

Autosomal dominant vitreoretinopathopathy (ADVIRC) is a rare condition first described by Kaufman et al.⁸ It has characteristic retinal and vitreous findings, in particular a peripheral retinal circumferential hyperpigmented band, punctate white opacities in the retina, vitreous fibrillar condensation, and breakdown of the blood retinal barrier with retinal neovascularization. Since its original description, the condition has been reported several times in families of diverse origin.⁹⁻¹¹ Importantly, EOG abnormalities in a subset of these families suggest that ADVIRC may represent a defect at the level of the RPE.¹² Most recently, Lafaut et al.¹³ reported a three-generation ADVIRC pedigree in which all affected members had the characteristic retinal findings and additionally had ocular developmental abnormalities including nanophthalmos, microcornea, closed angle glaucoma, and congenital cataract.

Using this family for genetic analysis, we established linkage of an ADVIRC phenotype to the pericentromeric region of chromosome 11. The disease locus in another family with a

From the ¹Academic Unit of Medical Genetics and Regional Genetics Service, St. Mary's Hospital, Manchester, United Kingdom; ²Department of Ophthalmology, Ghent University Hospital, Ghent, Belgium; ³Centre for Medical Genetics, Ghent University Hospital, Ghent, Belgium; ⁴Department of Ophthalmology, St-Jan General Hospital, Bruges, Belgium; ⁵Institute of Ophthalmology, London, United Kingdom; ⁶Department of Ophthalmic Research, Cole Eye Institute, Cleveland, Ohio; ⁷Department of Medical Genetics, Addenbrookes Hospital, Cambridge, United Kingdom; ⁸Exploration Fonctionnelle de la Vision, Centre Hospitalier Régional Universitaire, Hôpital Roger Salengro, Lille Cedex, France; ⁹Academic Department of Ophthalmology, Manchester Royal Eye Hospital, Manchester, United Kingdom; ¹⁰Centre for Molecular Medicine, University of Manchester, Manchester, United Kingdom.

²These authors contributed equally to the work presented here and should be regarded as equivalent senior authors.

Supported by Grant GR067443AIA from the Wellcome Trust (RP, JY). GCMB is a Wellcome Trust Senior Research Fellow in Clinical Science.

Submitted for publication May 18, 2004; accepted June 28, 2004.

Disclosure: **J. Yardley**, None; **B.P. Leroy**, None; **N. Hart-Holden**, None; **B.A. Lafaut**, None; **B. Loeys**, None; **L.M. Messiaen**, None; **R. Perveen**, None; **M.A. Reddy**, None; **S.S. Bhattacharya**, None; **E. Traboulsi**, None; **D. Baralle**, None; **J.-J. De Laey**, None; **B. Puech**, None; **P. Kestelyn**, None; **A.T. Moore**, None; **F.D.C. Manson**, None; **G.C.M. Black**, None

The publication costs of this article were defrayed in part by page charge payment. This article must therefore be marked "advertisement" in accordance with 18 U.S.C. §1734 solely to indicate this fact.

Corresponding author: Graeme C. M. Black, Department of Clinical Genetics, St Mary's Hospital, Hathersage Road, Manchester M13 0JH, UK; gblack@man.ac.uk.

related autosomal dominant phenotype comprising microcornea, rod-cone dystrophy, cataract, and posterior staphyloma (MRCS) also maps to this region.¹⁴ Analysis of these two families, and a further three families with similar developmental eye abnormalities and retinal dystrophy, showed that all affected members had pathogenic alterations that cause simultaneous missense substitutions and exon skipping in *VMD2*. Until now *VMD2* was regarded as a gene that underlies Best disease, a macular dystrophy which leads to loss of vision postdevelopmentally. The data demonstrated that *VMD2* mutations also underlie defects of ocular patterning, thereby supporting the hypothesized role for the RPE, and specifically *VMD2*, in the normal growth and development of the eye.

METHODS

Linkage Analysis

Genomic DNA from 13 members of Family 1 was amplified for known polymorphic genetic markers. The research followed the tenets of the Declaration of Helsinki and informed consent was obtained from the subjects after explanation of the nature and possible consequences of the study. PCR reactions with Abgene Reddymix *Taq* (Abgene, Epsom, UK) contained 50 ng genomic DNA in a final volume of 30 μ L and was amplified as follows: 95°C for 5 minutes, followed by 30 cycles of 94°C for 30 seconds; x° C for 30 seconds; 72°C for 30 seconds (where x° C is the primer annealing temperature). Final extension was carried out at 72°C for 10 minutes. The PCR product (5 μ L) was mixed with 5 μ L of formamide loading dye, denatured at 96°C for 5 minutes, and separated on a Sequagel 8 (National Diagnostics, Hesse, UK) denaturing PAGE run at 400 V for 3 hours at 20°C and silver stained using standard methods.

Locations and marker order for chromosomes 5, 11, and 12 were taken from <http://genome.ucsc.edu> and the Genome Database (www.gdb.org). For linkage analysis, allele frequencies were used from the Genome Database. Two-point Lod scores were calculated using the MLINK package.¹⁵

DNA Sequencing

Primers were designed to amplify all coding exons including 50 to 100 bp of flanking intron sequence of *VMD2* (sequence obtained from <http://genome.ucsc.edu/>; primers available on request). These primers were used initially to amplify genomic DNA from two affected individuals in Family 1 and an unaffected control. After sequencing (see below) and the identification of a possible disease causing mutation, DNA from other family members was amplified to confirm co-segregation. PCR reactions using Abgene Reddymix *Taq* (Abgene) contained 50 ng genomic DNA in a volume of 30 μ L and were cycled as described in the Linkage Analysis section. PCR products were purified using Microcon columns (Millipore, Watford, UK) according to the manufacturer's instructions.

Standard cycle sequencing reactions using BigDye terminator mix v1.1 (Applied Biosystems, Warrington, UK) contained 3–10 ng purified PCR product in 10 μ L and were performed using the forward and reverse primers used for initial amplification. The sequencing reactions were then precipitated, dried, and analyzed on an ABI 3700 capillary sequencer (ABI, Foster City, CA).

The exonic regions of *VMD2* were analyzed by sequencing in Families 2 to 5 and by SSCP in 68 unrelated individuals with anterior segment dysgenesis, respectively. The absence of any disease causing mutations from control individuals was confirmed by either single-stranded conformational polymorphism (SSCP) analysis or restriction digest. For SSCP/heteroduplex analysis, 5 μ L PCR product was mixed with 5 μ L of formamide loading dye, denatured, and separated on an 8% acrylamide/bis-acrylamide gel run at 350 V for 16 hours at 4°C and silver stained using standard methods.¹⁶

Cloning

Primers containing a 5' *NdeI* site were designed to amplify the exon of interest and to include approximately 250 bp of flanking intron on either side. Amplification of genomic DNA from affected individuals was carried out by PCR with Abgene Reddymix HiFidelity *Taq* (Abgene) containing 40 ng genomic DNA in 20 μ L. PCR reaction products were cloned into the TA cloning vector pCRII (Invitrogen, Paisley, UK) as per the manufacturer's instructions. Clones carrying either the mutant or wild-type allele were identified by direct sequencing. Both wild-type and mutant alleles were subcloned as *NdeI* fragments into a modified version of the α -globin-fibronectin-EDB minigene as described previously.¹⁷

Expression of Minigene

Plasmid (0.4 μ g) was transfected into lens cell line CRL-11421 and into human embryological kidney CRL-1573 cells (ATCC, Teddington, UK) using Effectene transfection reagent (Qiagen, Crawley, UK) as per the manufacturer's instructions. Cells were seeded at 2×10^5 per well in 6-well plates 24 hours before transfection. Twenty-four hours after transfection, total RNA was extracted from cells using Trizol reagent (Invitrogen) according to the manufacturer's instructions. RT-PCR reactions were performed using the One-Step RT-PCR system (Invitrogen) according to the manufacturer's instructions with minigene-specific primers or a combination of minigene- and *VMD2*-specific primers. PCR products were analyzed by agarose gel electrophoresis.

RESULTS

Clinical Details

The five families under study all had autosomal dominant developmental eye abnormalities (including nanophthalmos, microcornea, closed angle glaucoma, and congenital cataract) associated with retinal dystrophy (Fig. 1). Families 1, 2, and 3 have been previously described.^{13,14,18} In all five families the retinal dystrophy was characteristic of ADVIRC with circumferential peripheral retinal hyperpigmentation, punctate retinal and vitreous opacities, and choroidal atrophy. Individuals from all families had abnormal electro-retinograms (ERG), suggestive of a more widespread photoreceptor dysfunction. Family 2 had a more severe retinal phenotype including rod-cone dystrophy and posterior staphyloma. Affected individuals in all families had pathologically low EOGs.

Genetic Analysis and Sequencing of *VMD2* in Families with Nanophthalmos and Retinal Dystrophy

The combined vitreous and retinal phenotype in Family 1 prompted an initial linkage study. Linkage exclusion (Lod score < -2) was confirmed for the regions surrounding COL2A1 and the WGN1 loci (D5S1726). Thereafter evidence of linkage to the exudative vitreoretinopathy (EVR1/EVR3) loci on chromosome 11 was sought and high Lod scores were obtained for the markers D11S4152 and D11S4200 ($Z_{\max} = 3.26$, $\theta = 0.0$; Fig. 2). Having demonstrated significant linkage to this region, refinement of the critical region was undertaken further using microsatellite markers (Fig. 2). Haplotype analysis delineated a region between the flanking markers D11S4152 and D11S4139 which delineates a region of around 38 cM (35 to 73 cM; Centre for Medical Genetics genetic map, Marshfield Medical Research Foundation, Marshfield, WI; Fig. 2).

The critical region identified in Family 1 overlapped the putative loci for two other ocular developmental disorders, autosomal dominant nanophthalmos (NNO1) and MRCS,^{14,19} and strongly suggested that there was a group of related phenotypes which mapped to the same region. The putative MRCS locus was previously localized to a 5 cM region flanked by the

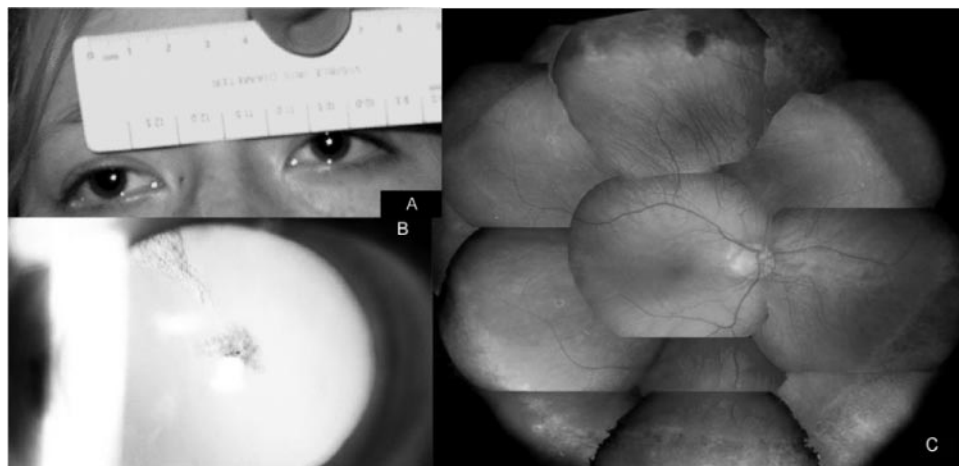
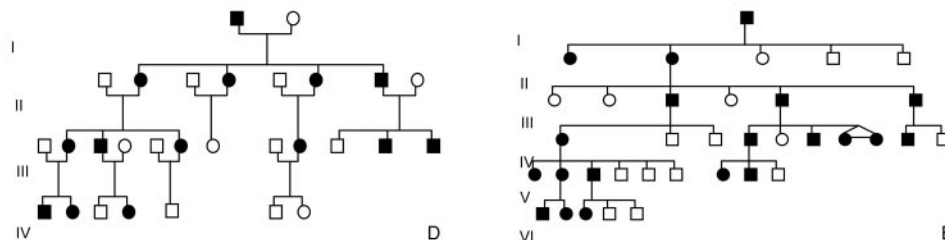


FIGURE 1. Clinical features of developmental phenotypes caused by mutation in *VMD2*. (A) Microcornea in individual VI₃ of Family 3. The horizontal corneal diameter demonstrated is 9.5 mm. (B) Posterior subcapsular cataract in individual III₆ of Family 1. (C) Fundal photomontage of individual VI₂ of Family 3. (D, E) Pedigrees of Family 1 and 3, respectively.



markers D11S4191 and D11S1883 in Family 2¹⁴. *VMD2* also lies within the regions delineated by the genetic analyses of all three diseases (ADVIRC, NNO1 and MRCS). Since affected individuals both Families 1 (ADVIRC) and 2 (MRCS) had pathologically low EOGs,¹³ a clinical finding also seen in Best macular dystrophy, we hypothesized that this phenotype resulted from a defect at the level of the RPE and may be due to a mutation in *VMD2*.

Sequencing of the *VMD2* coding sequence in Family 1 (of Belgian origin) revealed a missense change resulting in the substitution of valine by methionine at codon 86 in exon 4 (c.256G>A, p.V86M; Fig. 3). Subsequent analysis of all *VMD2* exons and introns in Families 2 to 5 revealed disease-causing sequence alterations in each (Fig. 3). The V86M substitution was also found in Family 3 (from NE France),¹⁸ and Family 4, (from Belgium, unpublished). Analysis with two intragenic microsatellite markers was consistent with this being a single ancestral mutational event in all three families (data not shown). Sequencing of affected individuals from Family 2 revealed an adenine to guanosine substitution at position 715 in exon 7 (c.715G>A, p.V239M) and a guanosine to adenine substitution at position 707 in exon 6 (c.707A>G, p.Y236C) in Family 5. All three sequence alterations fully co-segregated with all affected family members and were not present in 400 normal control chromosomes. Screening of *VMD2* in 18 unrelated individuals with microphthalmia/coloboma and 50 individuals with various forms of anterior segment dysgenesis revealed no pathogenic alterations.

Splicing Assays for Novel *VMD2* Mutations

The sequence alterations in Families 1 to 5 resulted in substitutions of conserved residues within transmembrane domains of bestrophin and may, therefore, be likely to have similar molecular consequences. None were previously described in association with Best disease, age-related macular disease (AMD), or as nonpathogenic variants. However all lie close to missense mutations that underlie Best disease (Y85H, V89A, V235L, V235M, T237R, T241N; www.uni-wuerzburg.de/human-genetics/vmd2.html). To explain how different phenotypes

can be caused by different closely-spaced missense mutations in the same gene, we hypothesized that the mutations in the present study might also affect splicing. Support for this hypothesis came from bioinformatic analysis using the ESEFinder program (<http://exon.cshl.org/ESE/>) which demonstrated that both V86M and Y236C may affect exonic splicing regulatory elements²⁰ (Table 1).

To test the effects on splicing of all three mutations, an *in vitro* functional assay was used that has demonstrated the effects of various splice site mutations in other genes.¹⁷ In this system the test exon and flanking intronic sequences are cloned into a fibronectin minigene to assay for the existence of splice sites. In all three cases there was a clear disruption of splicing (Fig. 4; Y236C, results not shown) that is likely to result in exonic skipping due to the altered binding of exon splicing modulators. This would produce an in-frame deletion in each case (Fig. 3). The possibility that similar Best disease-causing mutations also affect splicing was considered. The assay was therefore performed for two *VMD2* mutations that are known to cause Best disease and which are in close proximity to two of the mutations in the present study (Best mutation c.253T>C close to c.256G>A and Best mutation c.727G>A close to c.715G>A). In all cases the presence of the ADVIRC-associated sequence alterations resulted in the creation of novel splice-forms that were specific to the constructs and were not found using exons that were either wild-type or contained Best disease-causing mutations (Fig. 3). The splicing assays were performed on at least three separate occasions and were performed in two different immortalized cell lines for the c.256G>A and c.715G>A sequence alterations.

DISCUSSION

In addition to causing Best disease, sequence alterations in *VMD2* were shown to cause ocular developmental abnormalities, including nanophthalmos associated with a generalized retinal dystrophy. The three sequence alterations presented here result in missense substitutions which we have shown also cause exon skipping in transcripts *in vitro*. It is therefore

MARKERS	
Distance from 11pter in cM	
D11S929	33
D11S4152	35
D11S4200	43
D11S905	52
D11S4076	62
D11S1883	65
D11S1889	67
D11S4178	68
D11S4139	73
D11S1362	84

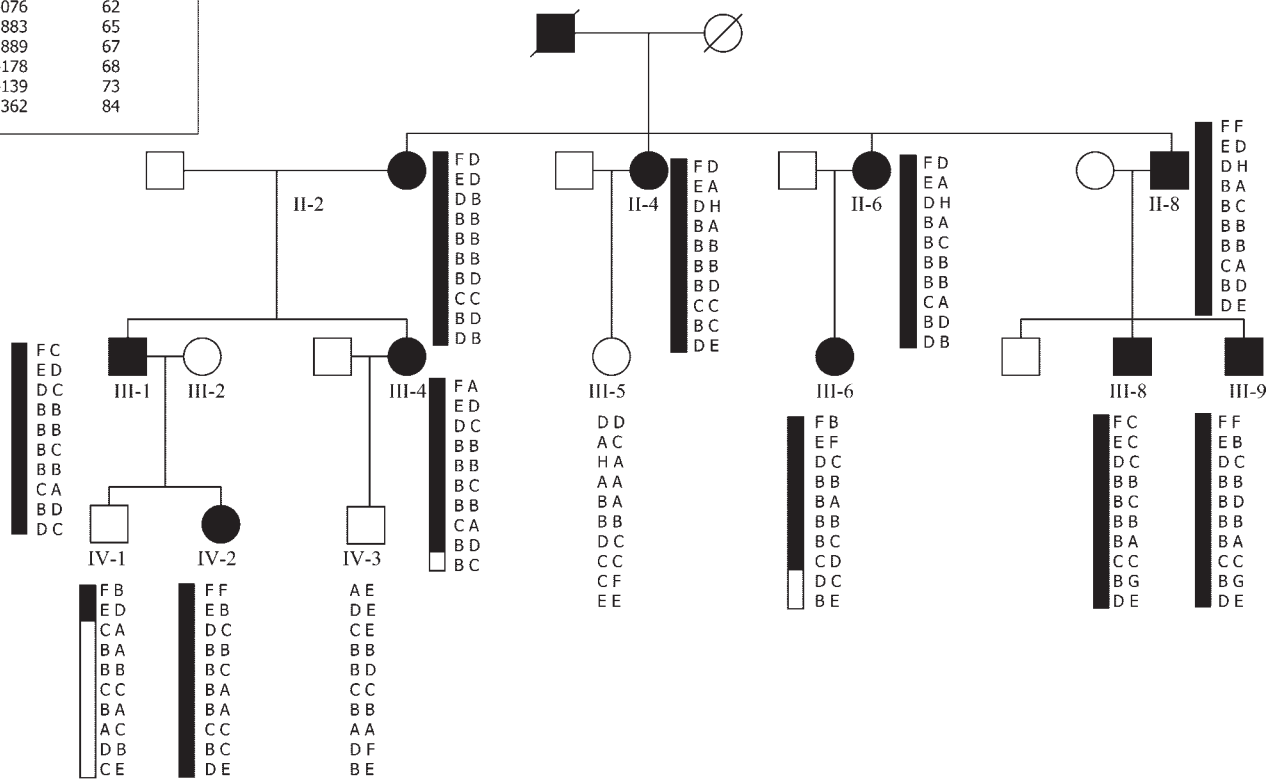


FIGURE 2. Genetic analysis of ADVIRC family 1 demonstrating haplotypes for markers from pericentric region of chromosome 11. Disease haplotype is indicated by *black line*. Multiple informative recombination events in individuals IV-1 and III-6 delineate a critical region flanked by markers D11S4152 and D11S4139.

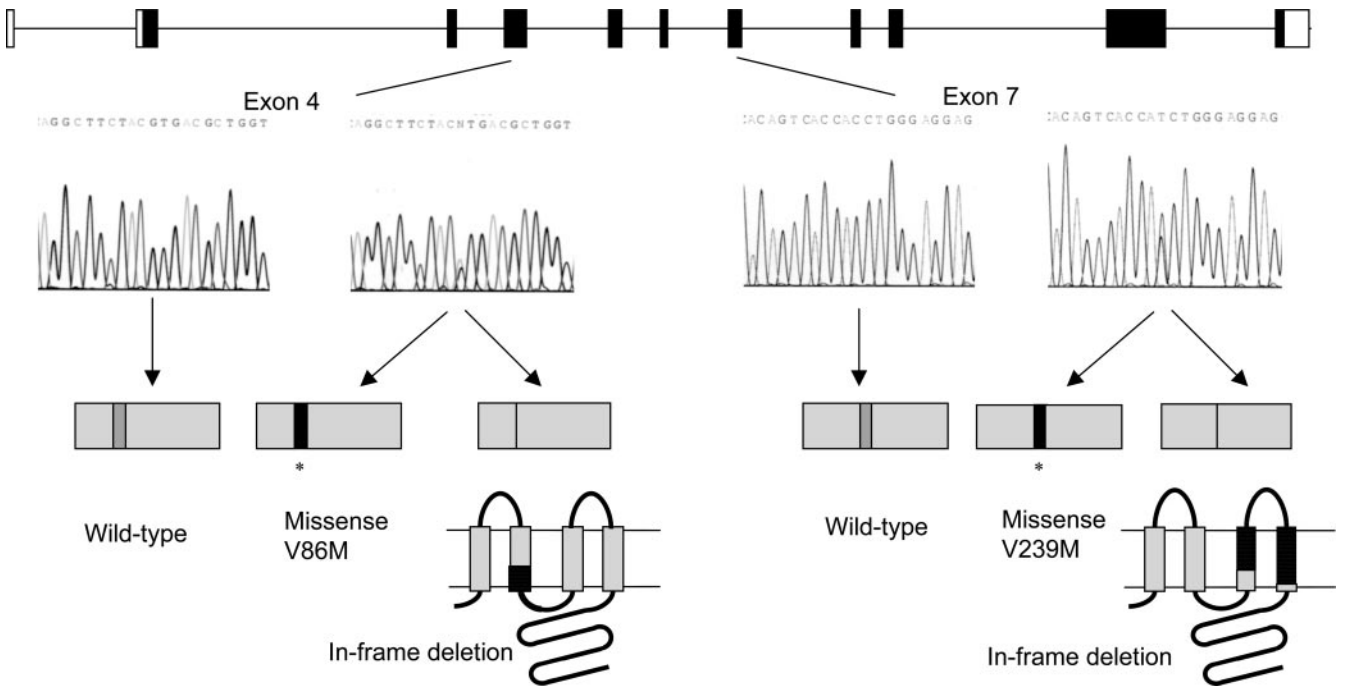


FIGURE 3. Ideogram showing effects of exon 4 and 7 mutations of *VMD2*. Exon 4 mutation on *left* (Families 1, 3, and 4), exon 7 mutation on *right* (Family 2). Sequence electropherograms showing wild-type (*left*) and mutant (*right*) sequences. Mutant sequences are shown in heterozygous state. For exon 7, reverse sequence is shown. Mutation results in the predicted expression of two protein isoforms, one containing a missense mutation, the other resulting in an in-frame deletion. The region of *VMD2* deleted is shown in black by a modeled diagram of *VMD2* (after Sun et al.⁵).

TABLE 1. Analysis of Mutational Effects on Exonic Splicing Enhancers

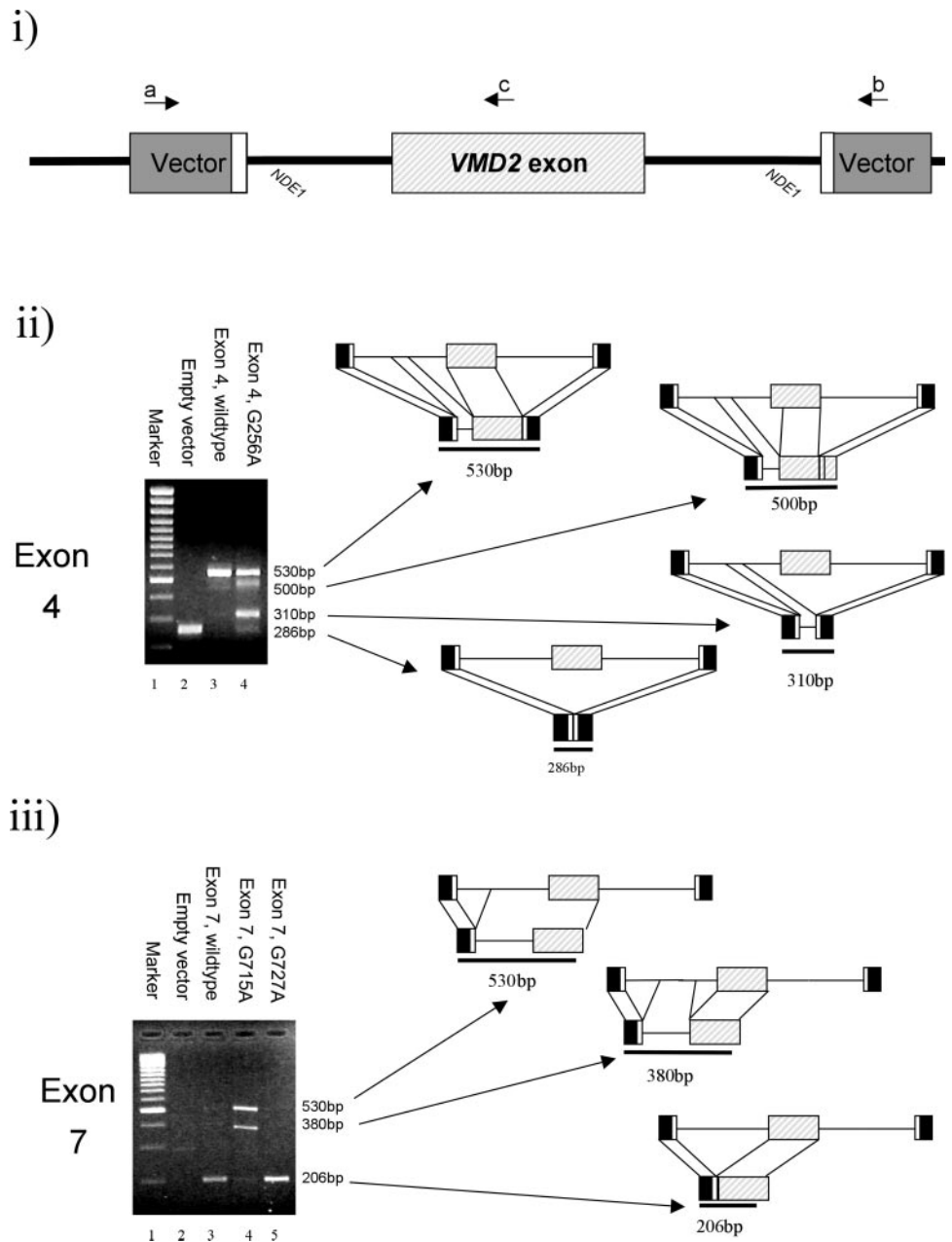
Mutation	Phenotype	ESEFinder Analysis
Y85H	Best	No major changes
V86M	Families 1,3 & 5	Creates site for SRp40
V89A	Best	Abolishes site for SF2/ASF
I232I	Neutral polymorphism	Abolishes site for SF2/ASF
Y236C	Family 4	Creates site for SC35

The effect of sequence changes on binding sites for the four splicing factors SF2/ASF, SC35, SRp40 and SRp55 were analyzed using the ESEFinder program.⁹ The Y85H, V89A and I232I changes were selected from the VMD2 database (www.uni-wuerzburg.de/humangenetics/vmd2.html) as changes with known phenotypic effects located close to the mutations in four of our families. ESEFinder gives indicative data, not definitive results.

likely that all three sequence alterations act through a similar mechanism. We also confirmed that sequence changes underlying Best disease which lie close to those described here do not cause exon skipping. This suggests a high degree of genotype-phenotype correlation for particular mutations in *VMD2*. The demonstration of disrupted splicing for all three mutations confirms the bioinformatic prediction that these sequence alterations alter exonic splicing regulatory elements.²⁰ In addition to exon skipping products, putative cryptic splice products were also observed, probably due to the artificial nature of the in vitro assay.

These data suggested that each heterozygous affected individual produces three bestrophin isoforms. In addition to the product of the wild-type allele, each mutant allele is capable of producing two abnormal proteins, one containing a missense substitution, the other an in-frame deletion. The different phenotypes, which in Family 2 was more severe than in the other families, are likely to relate the different properties and pro-

FIGURE 4. In vitro splicing assay using minigene constructs containing wild-type and mutant *VMD2* exons. Wild-type and mutant forms of exons 4 and 7 were cloned into a minigene vector and transfected into mammalian cells.¹⁷ After extraction, RNA was reverse-transcribed to assay the effects of *VMD2* mutations on splicing. (i) Diagram of splicing assay construct showing position of primers used for PCR. (ii) Splicing analysis of *VMD2* exon 4 G256A mutation. PCR used vector-specific primers (a) and (b). Lane 1: molecular marker; Lane 2: control minigene without *VMD2* exon shows amplification of 286 bp band corresponding to spliced vector exons; Lane 3: minigene containing wild-type exon 4. The 530 bp band corresponds to normally spliced *VMD2* exon 4; Lane 4: minigene containing exon 4 with G256A mutation. In addition to 530 bp band, there is now a small proportion of the 286 bp band (corresponding to skipping of *VMD2* exon 4) and two additional bands which sequencing corresponded to splice-forms using alternative upstream splice sites present in the minigene construct. RT-PCR using GAPDH was used to normalize the reactions. (iii) Splicing analysis of *VMD2* exon 7 G715A mutation. PCR used vector-specific primer (a) and *VMD2*-specific primer (c). Lane 1: molecular marker; Lane 2: control minigene without *VMD2* exon; Lane 3: minigene containing wild-type exon 7. Band of 206 bp corresponds to normally spliced *VMD2* exon 7; Lane 4: minigene containing exon 7 with G715A mutation. There is only a very low level of the 206 bp band, suggesting that the mutation severely disrupts splicing. As in (ii), there are additional bands corresponding to splice-forms using alternative upstream splice sites present in the minigene construct but not in human genomic DNA. Lane 5: minigene containing Best-disease causing mutation G727A. Band of 206 bp corresponds to normally spliced *VMD2* exon.



portions of the two mutant (i.e., substituted and truncated) isoforms. A similar mechanism was proposed by Zenker et al.²¹ for a patient with dual phenotypes (periventricular nodular heterotopia and frontometaphyseal dysplasia) that are presumed to result from the presence of dual isoforms of filamin a (FLNA) that are both produced by a de novo mutation which results in both exon skipping and a missense substitution. The illustration that a pathogenic missense mutation may also alter the regulation of splicing is likely to be a widely applicable disease mechanism for other disorders. It is likely that other missense substitutions within exons, in particular those altering exonic splicing regulatory elements, will also specific phenotypic consequences.

Ninety of 93 identified *VMD2* mutations in patients with classical Best disease are missense mutations or small in-frame deletions (www.uni-wuerzburg.de/humangenetics/vmd2.html and Ref. 7). The others consist of a splice site mutation and two frameshift mutations, one of which affects the extreme C terminus of the protein. One patient who is homozygous for the mutation W93C had a phenotype consistent with Best disease.^{4,22} However, haploinsufficiency may result in a different phenotype. Since bestrophin acts as an oligomer,⁵ there is scope for dominant negative effects. We suggest that the abnormally spliced products described here have a novel deleterious effect on ocular development. Since individuals in all four families had clinical and developmental features of nanophthalmos, this suggests that a mutation of *VMD2* could also underlie the original NNO1 family which has been mapped to a critical region encompassing the gene.¹⁹

The RPE is critical to ocular patterning, and its early ablation leads to arrest of eye growth and subsequent resorption of all ocular structures.¹ Within the eye *VMD2* is expressed in both developing and adult RPE.^{4,23} Although the mechanism underlying the developmental defects in the families presented here remains to be elucidated, our data support the hypothesized role for the RPE in ocular growth. Interestingly, the MITF transcription factor that is crucial for RPE differentiation and maintenance, and that is mutated in the *microphthalmia* mouse, regulates the expression of *VMD2*.²⁴ The maintenance and health of the RPE is central to photoreceptor maintenance and to the pathogenesis of AMD, a disease that shares several characteristics with Best disease. It is unknown why patients with these mutations have evidence of a predominantly peripheral retinal phenotype and generalized photoreceptor cell death (as witnessed by the intraretinal pigment and abnormal ERGs), while patients with Best disease have cell death confined to the macular region. Until now, *VMD2* has been regarded as the gene that underlies Best disease, a macular dystrophy that leads to loss of vision later in life. The observed defects of ocular growth (nanophthalmos) as a result of mutations in *VMD2* therefore potentially demonstrate a common etiology for pathologic processes of development and of later-onset (macular dystrophy).

Many genes underlying ocular developmental disorders also encode proteins expressed postdevelopmentally, for example, microphthalmia (*SOX2*, *CHX10*, *MITF*),^{2,25,26} anterior segment dysgenesis (*MAF*, *PITX2*),^{27,28} glaucoma (*LMX1B*, *MYOC*),^{29,30} and congenital cataract (*PITX3*, *PAX6*).^{31,32} In the case of both *MAF* and *PAX6*, pathogenic mutations are known to cause both congenital (cataract and aniridia, respectively) and late-onset (progressive cortical cataract and keratitis, respectively) phenotypes in the same individuals.³³ Such proteins have important roles in both the development and maintenance of mature tissues. In the context of identifying candidates for multifactorial late-onset disorders, our data suggest that the distinction between 'developmental' and 'late-onset' genes is artificial and that developmental genes with appropriate tissue expression

should be considered as candidate genes for late-onset disorders.

Electronic Database Information

VMD2 sequence alterations: www.uni-wuerzburg.de/humangenetics/vmd2.html. Locations and marker order for chromosomes University of California Santa Cruz (<http://genome.ucsc.edu>) and the Genome Database (www.gdb.org). ESEFinder program (<http://exon.cshl.org/ESE/index.html>).

References

1. Raymond SM, Jackson IJ. The retinal pigmented epithelium is required for development and maintenance of the mouse neural retina. *Curr Biol*. 1995;5:1286-1295.
2. Steingrimsson E, Moore KJ, Lamoreux ML, et al. Molecular basis of mouse microphthalmia (mi) mutations helps explain their developmental and phenotypic consequences. *Nat Genet*. 1994;8:256-263.
3. Boulton M, Dayhaw-Barker P. The role of the retinal pigment epithelium: topographical variation and ageing changes. *Eye*. 2001;15:384-389.
4. Petrukhin K, Koisti MJ, Bakall B, et al. Identification of the gene responsible for Best macular dystrophy. *Nat Genet*. 1998;19:241-247.
5. Sun H, Tsunenari T, Yau KW, et al. The vitelliform macular dystrophy protein defines a new family of chloride channels. *Proc Natl Acad Sci*. 2002;19:4008-4013.
6. Tsunenari T, Sun H, Williams J, et al. Structure-function analysis of the bestrophin family of anion channels. *J Biol Chem*. 2003;278:41114-41125.
7. Kramer F, Mohr N, Kellner U, et al. Ten novel mutations in *VMD2* associated with Best macular dystrophy (BMD). *Hum Mutation*. 2003;22:418-424.
8. Kaufman SJ, Goldberg MF, Orth DH, et al. Autosomal dominant vitreoretinopathopathy. *Arch Ophthalmol*. 1982;100:272-278.
9. Blair NP, Goldberg MF, Fishman GA, et al. Autosomal dominant vitreoretinopathopathy (ADVIRC). *Br J Ophthalmol*. 1984;68:2-9.
10. Traboulsi EI, Payne JW. Autosomal dominant vitreoretinopathopathy. Report of the third family. *Arch Ophthalmol*. 1993;111:194-196.
11. Goldberg MF, Lee FL, Tso MO, et al. Histopathologic study of autosomal dominant vitreoretinopathopathy. Peripheral annular pigmentary dystrophy of the retina. *Ophthalmology*. 1989;96:1736-1746.
12. Han DP, Lewandowski MF. Electro-oculography in autosomal dominant vitreoretinopathopathy. *Arch Ophthalmol*. 1992;110:1563-1567.
13. Lafaut BA, Loeys B, Leroy BP, et al. Clinical and electrophysiological findings in autosomal dominant vitreoretinopathopathy: report of a new pedigree. *Graefes Arch Clin Exp Ophthalmol*. 2001;239:575-582.
14. Reddy MA, Francis PJ, Berry V, et al. A clinical and molecular genetic study of a rare dominantly inherited syndrome (MRCS) comprising of microcornea, rod-cone dystrophy, cataract, and posterior staphyloma. *Br J Ophthalmol*. 2003;87:197-202.
15. Lathrop GM, Lalouel JM, Julier C, et al. Strategies for multilocus linkage analysis in humans. *Proc Natl Acad Sci USA*. 1984;81:3443-3446.
16. Sambrook J, Russell D. *Molecular cloning. A laboratory manual*. 3rd ed. New York: Cold Spring Harbor Laboratory Press; 2000.
17. Baralle M, Baralle D, De Conti L, et al. Identification of a mutation that perturbs NF1 gene splicing using genomic DNA samples and a minigene assay. *J Med Genet*. 2003;40:220-222.
18. François P, Puech B, Hache JC, et al. Hérédo-dystrophie chorioretinovitreuse, microcornée, glaucome et cataracte. *J Fr Ophthalmol*. 1993;16:129-140.
19. Othman MI, Sullivan SA, Skuta GL, et al. Autosomal dominant nanophthalmos (NNO1) with high hyperopia and angle-closure

- glaucoma maps to chromosome 11. *Am J Hum Genet.* 1998;63:1411-1418.
20. Cartegni L, Wang J, Zhu Z, et al. ESEfinder: A web resource to identify exonic splicing enhancers. *Nucleic Acids Res.* 2003;31:3568-3571.
 21. Zenker M, Rauch A, Winterpacht A, et al. Dual phenotype of periventricular nodular heterotopia and frontometaphyseal dysplasia in one patient caused by a single FLNA mutation leading to two functionally different aberrant transcripts. *Am J Hum Genet.* 2004;74:731-737.
 22. Nordström S, Thorburn W. Dominantly inherited macular degeneration (Best's disease) in a homozygous father with 11 children. *Clin Genet.* 1980;18:211-221.
 23. Bakall B, Marmorstein LY, Hoppe G, et al. Expression and localization of bestrophin during normal mouse development. *Invest Ophthalmol Vis Sci.* 2003;44:3622-3628.
 24. Esumi N, Oshima Y, Li Y, Campochiaro PA, Zack DJ. Analysis of the VMD2 promoter and implication of E-box binding factors in its regulation. *J Biol Chem.* 2004;30:279:19064-19073.
 25. Fantes J, Ragge NK, Lynch SA, et al. Mutations in SOX2 cause anophthalmia. *Nat Genet.* 2003;33:461-463.
 26. Percin EF, Ploder LA, Yu JJ, et al. Human microphthalmia associated with mutations in the retinal homeobox gene CHX10. *Nat Genet.* 2000;25:397-401.
 27. Jamieson RV, Perveen R, Kerr B, et al. Domain disruption and mutation of the bZIP transcription factor, MAF, associated with cataract, ocular anterior segment dysgenesis and coloboma. *Hum Mol Genet.* 2002;11:33-42.
 28. Semina EV, Reiter R, Leysens NJ, et al. Cloning and characterization of a novel bicoid-related homeobox transcription factor gene, RIEG, involved in Rieger syndrome. *Nat Genet.* 1998;14:392-399.
 29. Dreyer SD, Zhou G, Baldini A, et al. Mutations in LMX1B cause abnormal skeletal patterning and renal dysplasia in nail patella syndrome. *Nat Genet.* 1998;19:47-50.
 30. Stone EM, Fingert JH, Alward WL, et al. Identification of a gene that causes primary open angle glaucoma. *Science.* 1997;275:668-670.
 31. Hanson IM, Fletcher JM, Jordan T, et al. Mutations at the PAX6 locus are found in heterogeneous anterior segment malformations including Peters' anomaly. *Nat Genet.* 1994;6:168-173.
 32. Semina EV, Ferrell RE, Mintz-Hittner HA, et al. A novel homeobox gene PITX3 is mutated in families with autosomal-dominant cataracts and ASMD. *Nat Genet.* 1996;19:167-170.
 33. Jamieson RV, Munier F, Balmer A, et al. Pulverulent cataract with variably associated microcornea and iris coloboma in a MAF mutation family. *Br J Ophthalmol.* 2003;87:411-412.